



# Thermite reaction synthesis of nano-sized NiAl reinforced FeNiCr–TiC composite coating

Wen-Jun Xi\*, Neng Li, Tao Zhang, Wei-Li Zhu, Hai-Zhou Guo

School of Materials Science and Engineering, Beihang University, Beijing 100191, PR China

## ARTICLE INFO

### Article history:

Received 5 July 2009

Received in revised form 16 March 2010

Accepted 18 March 2010

Available online 25 March 2010

### Keywords:

Thermite reaction

Composite coating

NiAl

TiC

## ABSTRACT

A new nano-sized NiAl reinforced FeNiCr–TiC composite coating was fabricated using a thermite reaction technique in centrifugal field. All of the consisted phases in the composite coating were obtained in situ from the reaction product melt. The microstructure investigation showed that the composite coating consisted of ferrite ( $\alpha$ -FeNiCr), NiAl and TiC. The NiAl phase appeared in whisker with a diameter of about 100 nm and it was coherent with the ferrite matrix. The present composite coating exhibited excellent oxidation resistance and the mass gain after 100 h isothermal exposure at 1000 °C in air was less than 1 mg/cm<sup>2</sup> which is about 1/130 of that for CrNi1Mo steel. The coating had a good wear resistance, its relative wear resistance was 30–40 to the CrNi1Mo steel substrate at room temperature. As compared to NiCr1Mo steel, a significant increase of the composite coating in wear resistance at high temperature was observed. The volumetric wear rate of the composite coating was only about 1/7 of that for the NiCr1Mo steel.

© 2010 Elsevier B.V. All rights reserved.

## 1. Introduction

The FeNiCr–TiC cermet has been widely used in the fields of wear resistance tools and coating materials due to its excellent combination of wear and high-temperature corrosion resistance. The FeNiCr–TiC coating usually been manufactured through plasma and thermal spraying techniques. However, these coatings have all shown some drawbacks such as weak bonding strength with substrates, presence of microcracks and microroids, which decrease to some extent the corrosion, ductility and impact resistance of coatings [1]. Additionally, the surface of TiC particle has been easily dirtied in the producing process, which causes the bonding strength of TiC with the metal matrix to reduce, thus leading to depression of the mechanical property of coating. As is well known, the properties of composites are influenced by the bonding strength and microstructure of interface between strengthening phase and matrix. If all the components of a composite were obtained from a high-temperature melt and the reinforced phases were produced in situ in the reaction product melt, the interface incompatibility of matrices with reinforcements could be eliminated by creating more thermodynamically stable reinforcements based on their nucleation and growth from parent matrix phase. Recently, thermite reactions have become important in the synthesis of refractory ceramic and composite materials [2–7].

In this paper, we used thermite reactions in centrifugal field to produce a nano-sized NiAl reinforced FeNiCr–TiC composite coating. All of the consisted phases in the composite were obtained from the reaction product melt, therefore, reinforced phases such as TiC and NiAl should have good compatibility and high bonding strength with the alloy matrix, which should be beneficial for improving the mechanical properties of coating. The choice of NiAl as a reinforced phase is based on the fact that the B2 structure NiAl is coherent with bcc ferrous alloy matrix [8]; moreover, it has advantages such as high melting point, exceptional high-temperature corrosion and its good wettability with titanium carbide.

## 2. Experimental

### 2.1. Preparation of coatings

A thermite powder mixture was prepared by blending Al, Fe<sub>2</sub>O<sub>3</sub>, NiO, Cr<sub>2</sub>O<sub>3</sub>, CrO<sub>3</sub>, TiO<sub>2</sub> (or Ti) and graphite powders. The composition of starting materials is given in Table 1. A low carbon steel (CrNi1Mo) pipe with an outer diameter of 76 mm and wall thickness of 5 mm and a length of 100 mm was mounted on a centrifugal machine. The low carbon steel pipe was loaded with the thermite powder mixture, which was immediately ignited by a tungsten filament once a given rotation velocity of the centrifugal machine was reached. During the reactions, the oxides were reduced by Al, resulting in formation of metal Fe, Ni, Cr, Ti and alumina (Al<sub>2</sub>O<sub>3</sub>). The adiabatic temperature was sufficiently high that all reacted products became liquid. Due to the centrifugal force field, the molten mixture of Fe, Ni, Cr, Al, Ti and C with a density higher than that of alumina flowed into the inner surface of the low carbon steel pipe and formed a FeNiCr–TiC composite coating layer. A slag layer contained alumina covered the composite coating layer due to its low density.

The phases and composition of the prepared coating were analyzed using X-ray diffraction (XRD) and electron probe microanalysis (EPMA). The morphology

\* Corresponding author. Fax: +86 1082339772.

E-mail address: [xiwj@buaa.edu.cn](mailto:xiwj@buaa.edu.cn) (W.-J. Xi).

**Table 1**  
Composition of starting materials.

| Molecular formula  | Fe <sub>2</sub> O <sub>3</sub> | Cr <sub>2</sub> O <sub>3</sub> | CrO <sub>3</sub> | NiO  | Al   | Ti  | C   |
|--------------------|--------------------------------|--------------------------------|------------------|------|------|-----|-----|
| Compositions (wt%) | 30.5                           | 12.0                           | 12.0             | 10.0 | 24.0 | 9.2 | 2.3 |

and structure of the coating were investigated with scanning electron microscopy (SEM) and transmission electron microscopy (TEM).

## 2.2. Oxidation behavior

Oxidation behavior was studied in air. The oxidation test coupons were 10 mm × 10 mm × 1 mm thick and the surfaces were polished with 800-grit emery paper. The mass change data after 100 h isothermal exposure at 1000 °C in air for the investigated composite and NiCr1Mo steel were measured using a Sartorius CP225D electronic balance with a sensitivity of 0.01 mg.

## 2.3. Wear test

Tribological properties for room temperature were performed on an MM-200 testing machine, using block and ring specimens under dry sliding. The test specimens were machined into blocks of size of 8 mm × 8 mm × 18 mm. The ring material of the wear couple was a GCr15 steel. An NiCr1Mo steel with a chemical composition of about Fe–0.35C–0.40Mn–0.30Si–1.5Cr–1.5Ni–0.25Mo (wt%) was used as the reference material. The wear conditions were 98 N normal load, 0.05 ms<sup>-1</sup> sliding speed and 750 m sliding distance. Wear mass losses of the composite and reference material were measured by a Sartorius CP225D electronic balance with an accuracy of 0.01 mg. Average mass loss of every three specimens under the same conditions was used as the ultimate mass loss.

Specimens with dimensions of 20 mm × 20 mm × 4 mm were machined from the samples for elevated temperature tribological testing. Tribological experiments were carried on a self-designed ball-on-block high-temperature tribological tester in air. The counterpart was a Si<sub>3</sub>N<sub>4</sub> ceramic ball which has a diameter of 10 mm. The load was 50 N, the rotating speed of block 500 rev min<sup>-1</sup> and the dwell time 40 min. The testing temperature was 1000 °C. The cross-section of the worn scar of the discs was measured using a surface profilometer. The volumetric wear rate  $W$  was calculate using Eq. (1), where  $S$  is the area of the cross-section,  $L$  is the length of the stroke,  $v$  is the rotating speed and  $t$  is the dwell time.

$$W = \frac{SL}{vt} \quad (1)$$

## 3. Results and discussion

### 3.1. Coating microstructure

Fig. 1 shows the SEM cross-sectional image from the composite coating. The thickness of the coating is about 1.5 mm and no visible interfacial line has been found between the coating and substrate, which indicates that the coating is metallurgically bonded with the steel substrate. The SEM micrographs of the coating are shown in Fig. 2, where the black phase is TiC and the gray is alloy matrix. The TiC phase appears in two morphologies, i.e. polygon

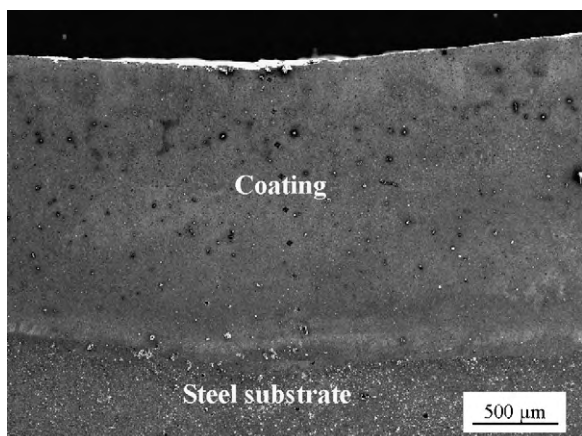


**Fig. 1.** SEM image of the cross-section of composite coating.

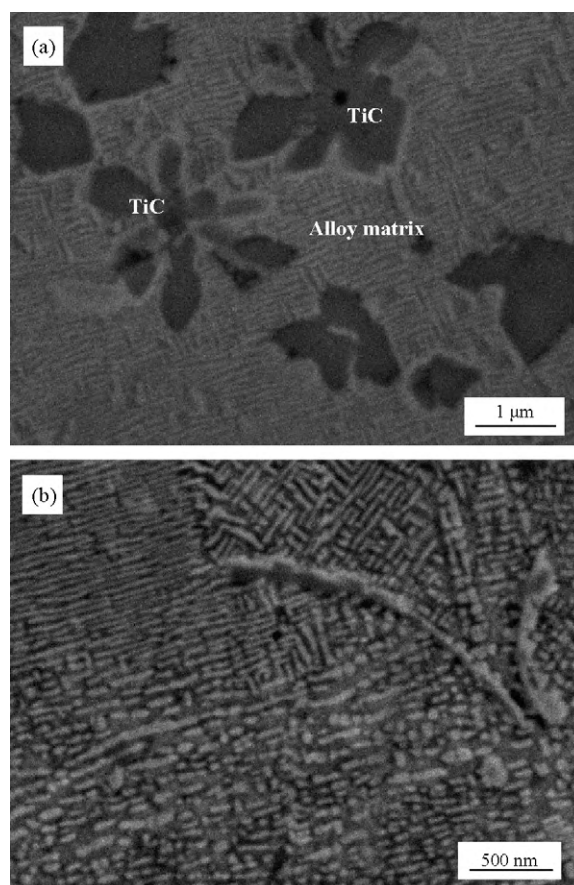


**Fig. 2.** SEM micrographs of the composite coating: (a) low magnification and (b) high magnification.

and flower-like with a range of grain size from 0.1 to 3 μm. The alloy matrix looks like wove cloth, in which thread-like grains have been close arranged, as shown in Fig. 2(a). A high magnification image of the matrix is shown in Fig. 2(b), it can be seen that rod-like grains grow parallelly to each other. The TEM results are shown in Fig. 3. The white flower-like phase is identified as TiC (Fig. 3(a)), the rod-like phase is NiAl with B2 ordered structure, and the matrix is bcc ferrite ( $\alpha$  phase) (Fig. 3(b)). The orientation relationship between the NiAl ( $\beta$  phase) and the ferrite has been determined to be  $(110)_{\beta} // (110)_{\alpha}$ ;  $[001]_{\beta} // [001]_{\alpha}$ . The B2 ordered structure of NiAl is a derivative of the bcc structure and its lattice parameter is 0.2880 nm which is close to that of  $\alpha$  ferrite (lattice parameter is 0.2876 nm) [9]. Therefore, NiAl should be coherent with  $\alpha$  matrix.

The grains of the alloy matrix and the NiAl phase are both fine in the composite coating. This suggests that the TiC grains precipitated first in the melt and then they became heterogeneous nucleation centers leading to significant increase of the nucleation rate of the alloy matrix. In addition, the centrifugal force made the alloy melt expand to a thin layer that kept close to the inner surface of steel tube and its heat was quickly adsorbed by the steel, and so it was solidified rapidly. Because of the great nucleation rate and rapid solidification, a remarkable grain refinement was produced in the alloy matrix. The nanosize NiAl with a diameter of about 100 nm was even obtained. On the other hand, both TiC and NiAl phases were produced in situ in the reaction melt, so they should have good interface compatibility and high bonding strength with the matrix. In particular, the coherent nano NiAl phase could generate more appreciable strengthening effect on the alloy matrix.

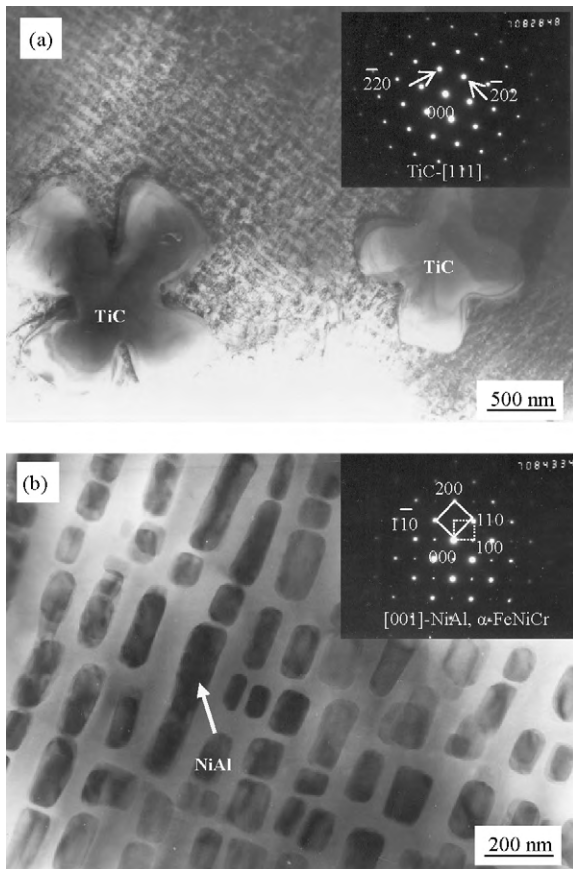


**Fig. 3.** TEM micrographs of the composite coating: (a) TiC in the alloy matrix, the inset is the selected-area diffraction pattern taken along the [1 1 1] zone axis of TiC and (b) NiAl precipitate in the  $\alpha$ -FeNiCr matrix, the inset displays the selected-area diffraction pattern taken along the [0 0 1] zone axis of NiAl and  $\alpha$ -FeNiCr.

### 3.2. Oxidation behavior

Fig. 4 shows the mass change data after 100 h isothermal exposure at 1000 °C in air for FeNiCr–TiC composite coating and CrNi1Mo steel. The XRD analysis of the surface of CrNi1Mo steel after exposing for 24 h in air indicated that the oxide layer on the surface was mainly  $\text{Fe}_2\text{O}_3$ . The CrNi1Mo steel exhibits very rapid weight change kinetics due to the formation of Fe-rich oxides on the surface. Above 30 h, however, the weight of CrNi1Mo steel specimen does not change because the whole specimen had been turned

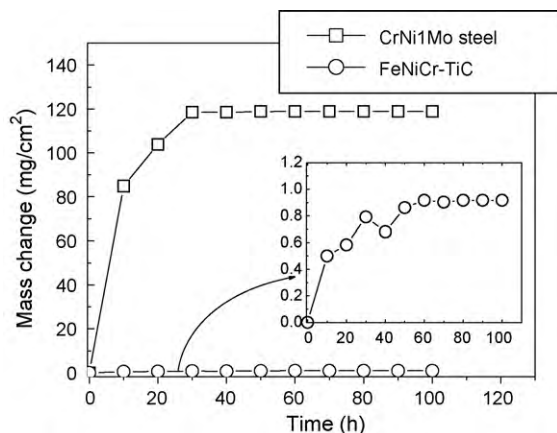


**Fig. 4.** The mass change data after 100 h isothermal exposure at 1000 °C in air for FeNiCr–TiC composite coating and CrNi1Mo steel.

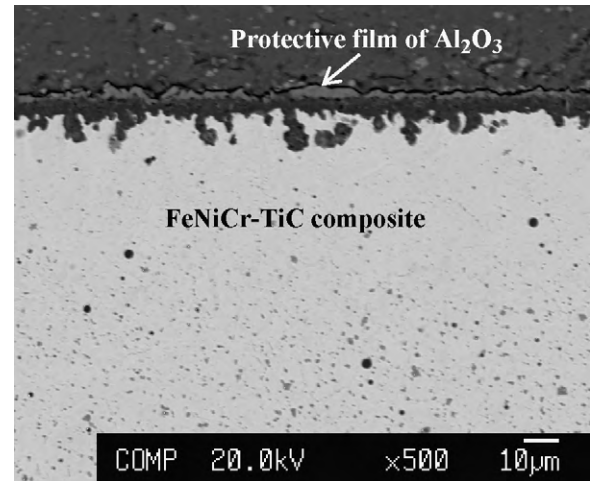


**Fig. 5.** SEM image of surface cross-sectional view of the FeNiCr–TiC composite.

**Table 2**

Compositional analysis of the oxidation layer of the FeNiCr–TiC composite by EPMA.

| Elements | O     | Al    | Fe   | Cr   | Ti   |
|----------|-------|-------|------|------|------|
| Weight % | 52.95 | 41.29 | 0.55 | 2.42 | 2.80 |
| Atomic % | 66.80 | 30.88 | 0.20 | 0.94 | 1.18 |

to oxides. The mass gain for CrNi1Mo steel after 100 h isothermal exposure at 1000 °C in air is about 119 mg/cm<sup>2</sup>. In contrast, the FeNiCr–TiC composite shows slow oxidation kinetics and its specific mass change obeys a parabolic growth rate only in the first 60 h of oxidation and then the mass change remains constant beyond 60 h. The mass gain of the composite is about 0.92 mg/cm<sup>2</sup> that is less than 1% of that for CrNi1Mo steel. Fig. 5 shows SEM image of surface cross-sectional view of the FeNiCr–TiC composite. The oxidation layer is continued and about 2 μm thick. The XRD analysis verified that the oxidation layer consisted of  $\text{Al}_2\text{O}_3$ ,  $\text{Cr}_2\text{O}_3$  and  $\text{Fe}_3\text{O}_4$ , after deducting the diffraction peaks of the matrix, such as  $\alpha$ -FeNiCr and NiAl. Compositional analysis by EPMA indicates that the surface is mainly composed of two elements of Al and O, with small amounts of Cr, Fe and Ti, as listed in Table 2. Combining the XRD results, we confirm that the oxidation layer is mainly composed of  $\text{Al}_2\text{O}_3$ . Therefore, the good oxidation resistance of the FeNiCr–TiC composite is associated to the formation of the protective film of  $\text{Al}_2\text{O}_3$  on the surface.

### 3.3. Wear resistance

The wear resistance of the coating was measured by using MM-200 wear tester under a dry sliding condition with a loading force of 98 N. The wear comparing specimen was cut from the carbon steel pipe and the friction material was GCr15 steel. The wear test shows that the FeNiCr–TiC composite coating has a good wear resistance, its relative wear resistance is 30–40 relative to the carbon steel. It is reasonable to assume there was a greater abrasion value in the alloy matrix than that in the TiC particles in the sliding wear process, the frictional element contacted mainly with the high hardness TiC particles, which resisted mainly the action of wear. Furthermore, the high bonding strength of TiC with the alloy matrix and good support to the TiC particles provided by the high strength of the alloy matrix would be all beneficial for increasing wear resistance of the coating.

The high-temperature tribological tests were carried in air at temperature 1000 °C for 40 min. The volumetric wear rate of the FeNiCr–TiC composite and the CrNi1Mo steel is  $4.80 \times 10^{-3} \text{ mm}^3/\text{m}$  and  $3.32 \times 10^{-2} \text{ mm}^3/\text{m}$ , respectively. The volumetric wear rate of

CrNi1Mo steel is found to be nearly seven times greater than that of FeNiCr–TiC composite, indicating that the FeNiCr–TiC composite has better wear resistance than CrNi1Mo steel at high temperature. It is possible that the TiC with a high melting point and high hardness played an important role to resist deformation and adhesive wear attacks effectively during the high-temperature wear test process. On the other hand, TiC particles form in situ in the melt of the composite, they have good compatibility and high bonding strength with the matrix, which is beneficial for improving the wear resistance at high temperature. The good high-temperature wear resistance of the composite is also due to good strength and toughness combination of  $\alpha$ -FeNiCr/NiAl matrix to a large extent. In addition, it may be attributed to excellent oxidation resistance of the composite at high temperature.

#### 4. Conclusions

It was shown that the NiAl nanowhiskers reinforced FeNiCr–TiC composite coating could be fabricated by thermite reaction synthesis. The composite coating consisted of ferrite ( $\alpha$ -FeNiCr), NiAl and TiC. The NiAl phase appeared in whisker with a diameter of about 100 nm and it was coherent with the ferrite matrix. The present composite coating exhibited excellent oxidation resistance and the

mass gain after 100 h isothermal exposure at 1000 °C in air was less than 1 mg/cm<sup>2</sup> which is about 1/130 of that for CrNi1Mo steel. The composite coating had an excellent high-temperature wear resistance. As compared to NiCr1Mo steel, the volumetric wear rate of the composite coating was only about 1/7 of that for NiCr1Mo steel.

#### Acknowledgment

This work was supported by National Natural Science Foundation of China (NSFC), Grant No. 50772007.

#### References

- [1] L. Pawlowski, *The Science and Engineering of Thermal Spray Coatings*, Wiley, New York, 1995.
- [2] A.G. Merzhanov, in: Z.A. Munir, J.B. Holt (Eds.), *Proceedings of Combustion and Plasma Synthesis of High-temperature Materials*, VCH Publishers, New York, 1990, pp. 1–53.
- [3] J.J. Moore, H.J. Feng, *Prog. Mater. Sci.* 39 (1995) 243–273.
- [4] O. Odawara, *J. Am. Ceram. Soc.* 73 (1990) 629–633.
- [5] L.L. Wang, Z.A. Munir, Y.M. Maximov, *J. Mater. Sci.* 128 (1993) 3693–3708.
- [6] W.J. Xi, S. Yin, H.Y. Lai, *J. Mater. Sci.* 35 (2000) 45–48.
- [7] W.J. Xi, S. Yin, H.Y. Lai, *J. Mater. Proc. Technol.* 137 (2003) 1–4.
- [8] H. Calderon, *M.E. Fine, Mater. Sci. Eng.* 63 (1984) 197–208.
- [9] JCPDS Cards No. 44-1188 and 34-0396.